

High-order harmonic generation by molecules of discrete rotational symmetry interacting with circularly polarized laser field

Vitali Averbukh,¹ Ofir E. Alon,¹ and Nimrod Moiseyev^{1,2}

¹*Department of Chemistry, Technion–Israel Institute of Technology, Haifa 32000, Israel*

²*Minerva Center for Non-Linear Physics of Complex Systems, Technion–Israel Institute of Technology, Haifa 32000, Israel*

(Received 14 March 2001; published 13 August 2001)

The dynamics of harmonic generation by a molecule of discrete rotational symmetry oriented in the polarization plane of a circularly polarized laser field is discussed. A simple model system is presented and the corresponding high-order harmonic generation spectrum is calculated analytically as a sum of the bound-bound and the bound-continuum contributions. It is shown that, contrary to the case of rare gas atoms interacting with linearly polarized radiation, the dominant contribution to high-order harmonic generation by the studied class of systems comes from the bound-bound transitions. As a consequence, the mechanism of the process is different from the well-known rescattering mechanism due to Corkum and Kulander. At intensities high enough the molecular harmonic generation spectra reproduce the main features of the atomic ones, i.e., the plateau and the cutoff. Unlike the cutoff in the atomic case, the molecular cutoff position depends linearly on the electric field strength and the molecular dimensions. This should allow one to reach higher harmonic orders by employing larger molecular targets.

DOI: 10.1103/PhysRevA.64.033411

PACS number(s): 33.80.Wz, 42.65.Ky, 42.25.Ja, 78.90.+t

I. INTRODUCTION

During the last decade great progress has been made in experimental and theoretical investigation of high-order harmonic generation (HHG) [1] aiming at the achievement of a small-size source of coherent radiation in the soft x-ray regime. Most of the studies have been concerned with generation of odd harmonics by rare gas atoms interacting with linearly polarized laser fields. The HHG spectrum of this system in the low-frequency–high-intensity regime consists of a plateau of length proportional to the ponderomotive energy and abrupt cutoff. The use of extremely short pulses has allowed experimentalists to extend the cutoff frequency up to the water window [2]. Development of phase matching techniques [3] has made it possible to increase the intensities of the emitted high harmonics by several orders of magnitude. The recent experimental successes make the application of high harmonics in spectroscopy and other areas a natural possibility (see, e.g., Ref. [4]).

One property that would make the harmonic radiation particularly useful is the selectivity of the HHG. The question is whether one can find a combination of an atomic or a molecular system and a laser field that would produce only several specific high harmonics. The issue of selectivity was addressed by Alon, Averbukh, and Moiseyev [5,6]. The authors presented a method for formulation of selection rules for HHG spectra and discussed a number of systems for which most of the harmonics are absent from the spectra for the symmetry reasons. Formulation of the selection rules requires three basic components: the Hamiltonian describing the system and its eigenfunctions, the symmetry operations commuting with the Hamiltonian and the matrix elements to be evaluated. A convenient formalism that allows us to pose the problem of the calculation of HHG spectra in terms of matrix elements and eigenfunctions is Floquet theory [7]. Indeed, within Floquet formalism the interaction of atoms

and molecules with laser fields is described by the Floquet Hamiltonian

$$\hat{\mathcal{H}}(t) = \frac{\hbar}{i} \frac{\partial}{\partial t} + \hat{H}(t), \quad (1)$$

where $\hat{H}(t)$ is the physical time-dependent Hamiltonian. The time-periodic part of the Floquet wave function is an eigenfunction of $\hat{\mathcal{H}}(t)$:

$$\hat{\mathcal{H}}(t)\Phi(t) = \varepsilon\Phi(t), \quad \Psi(t) = e^{-i\varepsilon t/\hbar}\Phi(t). \quad (2)$$

Moreover, the well-known dipole expression giving the amplitude of the n th harmonic of the incident radiation frequency ω as the corresponding Fourier component of the time-dependent dipole moment $\vec{\mu}(t)$,

$$\vec{A}_n \propto n^2 \int_0^{2\pi/\omega} dt e^{-in\omega t} \int_{-\infty}^{\infty} d\vec{r} \Phi^*(\vec{r}, t) \hat{\vec{\mu}} \Phi(\vec{r}, t), \quad (3)$$

can be easily represented as a matrix element:

$$\vec{A}_n \propto n^2 \langle\langle \Phi(\vec{r}, t) | \hat{A}_n | \Phi(\vec{r}, t) \rangle\rangle, \quad \hat{A}_n = \hat{\vec{\mu}} e^{-in\omega t}, \quad (4)$$

where the double bra-ket notation $\langle\langle \cdot \cdot \cdot \rangle\rangle$ means integration over space and time. The matrix element of Eq. (4) is a diagonal one, i.e., the bra and the ket are represented by the same quasienergy state. The nondiagonal matrix elements involving two different Floquet states correspond to the hyper-Raman lines and not to exact harmonics, unless an accidental degeneracy is present [8]. If the Floquet Hamiltonian is invariant under a transformation of space and time, i.e., it possesses a dynamical symmetry (DS)

$$\hat{P} \hat{\mathcal{H}}(t) \hat{P}^{-1} = \hat{\mathcal{H}}(t), \quad (5)$$

then the emitted harmonics are those for which at least one of the operators $\hat{A}_{j,n}$, $j=x,y,z$, is invariant under \hat{P} .

Using the method described above, the authors have shown, for example, that molecules of N th-order rotational symmetry, e.g., benzene, interacting with circularly polarized light emit under specific conditions only the first and the $(lN \pm 1)$ th high-order harmonics ($l=1,2,3,\dots$) of the incident radiation frequency [5]. The $1, lN \pm 1$ selection rule in this case is a consequence of the N th-order DS. DS is present in the system only if the molecular plane coincides with the polarization plane of the incident beam. Consequently, the experimental realization of the above DS requires molecular alignment. Very recently, there has been substantial experimental progress in the alignment of molecules with intense nonresonant laser fields [9]. This technique will probably allow researchers to perform multiphoton ionization and HHG experiments with aligned aromatic molecules in the near future.

The discussion of selectivity in HHG has been limited so far almost entirely to formulation of the selection rules. However, the DS considerations of Refs. [5,6,10] cannot predict the relative intensities of the symmetry-allowed harmonics. In order to get a full physical picture of HHG by systems possessing DS, one should investigate the underlying dynamics. The systems giving rise to selective HHG spectra do not possess a common physics, but rather have similar DS properties. The present study is confined to harmonic generation by rotationally symmetric target systems, such as aromatic molecules, interacting with a circularly polarized field. We will assume that the rotational symmetry axis is aligned along the propagation direction of the laser field. The dipole approximation with respect to both the incident and the emitted radiation will be used throughout this work.

In the following section we will present the harmonic amplitudes of such systems as a sum of the bound-bound and bound-continuum contributions. Section III will be devoted to the description of the bound-bound contribution by means of a simple N -level model, N being the order of rotational symmetry of a particular molecule. We will evaluate the bound-continuum contribution within the flat continuum approximation in Sec. IV, showing that it is much smaller than the bound-bound one for all the emitted harmonics. The implications of our results for the possibility of both effective and selective HHG by molecular targets will be discussed in the Conclusions.

II. BOUND-BOUND AND BOUND-CONTINUUM CONTRIBUTIONS TO THE HHG SPECTRUM

Let us describe the interaction of a molecule with a circularly polarized electric field $\vec{E}(t)$ in the length gauge, in the single-active-electron picture:

$$i\hbar \frac{\partial}{\partial t} \Psi(\vec{r}, t) = \hat{H} \Psi(\vec{r}, t), \quad \hat{H} = \frac{\hat{p}^2}{2m} + V(\vec{r}) - e\vec{E}(t) \cdot \vec{r}, \quad (6)$$

where m and e are the electron mass and charge and $V(\vec{r})$ is

the effective potential due to the interaction with the nuclei and other electrons, possessing a rotational symmetry axis of order N ,

$$\hat{C}_N V(\vec{r}) \hat{C}_N^{-1} = V(\vec{r}). \quad (7)$$

We assume that the C_N symmetry axis is perpendicular to the polarization plane of $\vec{E}(t)$.

The objective of our calculation is the time-dependent dipole moment. According to the selection rules for HHG spectra [5], the harmonics emitted by the molecule interacting with the circularly polarized field are also polarized circularly either like the incident radiation or in the opposite direction. Consequently, the important components of the induced molecular dipole moment are

$$\mu_{\pm}(t) = e \int_{-\infty}^{\infty} d^3r \Psi^*(\vec{r}, t) (x \pm iy) \Psi(\vec{r}, t). \quad (8)$$

The wave function of the system can be conveniently represented as a linear combination of the eigenfunctions of the molecular Hamiltonian \hat{H}_0 :

$$\begin{aligned} \Psi(\vec{r}, t) &= \sum_{j=1}^{\infty} a_j(t) \phi_j(\vec{r}) + \int_{-\infty}^{\infty} \frac{d^3p}{(2\pi\hbar)^3} b(\vec{p}, t) \varphi_{\vec{p}}(\vec{r}), \\ \hat{H}_0 \phi_j(\vec{r}) &= E_j \phi_j(\vec{r}), \quad \hat{H}_0 \varphi_{\vec{p}}(\vec{r}) = \frac{p^2}{2m} \varphi_{\vec{p}}(\vec{r}), \\ \langle \phi_j(\vec{r}) | \phi_k(\vec{r}) \rangle &= \delta_{j,k}, \quad \langle \phi_j(\vec{r}) | \varphi_{\vec{p}}(\vec{r}) \rangle = 0, \\ \langle \varphi_{\vec{p}}(\vec{r}) | \varphi_{\vec{p}'}(\vec{r}) \rangle &= (2\pi\hbar)^3 \delta(\vec{p} - \vec{p}'), \end{aligned} \quad (9)$$

where $a_j(t)$ and $b(\vec{p}, t)$ are the amplitudes of the bound $\phi_j(\vec{r})$ and continuum, $\varphi_{\vec{p}}(\vec{r})$ states with energies E_j and $p^2/2m$, respectively.

Substituting the expansion (9) into Eq. (8), one obtains

$$\begin{aligned} \mu_{\pm}(t) &= e \sum_{j,j'=1}^{\infty} a_j^*(t) \langle \phi_j | x \pm iy | \phi_{j'} \rangle a_{j'}(t) \\ &+ e \sum_{j=1}^{\infty} \int_{-\infty}^{\infty} \frac{d^3p}{(2\pi\hbar)^3} \{ a_j^*(t) \langle \phi_j | x \pm iy | \varphi_{\vec{p}} \rangle b(\vec{p}, t) \\ &+ b^*(\vec{p}, t) \langle \varphi_{\vec{p}} | x \pm iy | \phi_j \rangle a_j(t) \} \\ &+ e \int_{-\infty}^{\infty} \frac{d^3p}{(2\pi\hbar)^3} \int_{-\infty}^{\infty} \frac{d^3p'}{(2\pi\hbar)^3} b^*(\vec{p}, t) \\ &\times \langle \varphi_{\vec{p}} | x \pm iy | \varphi_{\vec{p}'} \rangle b(\vec{p}', t). \end{aligned} \quad (10)$$

The above equation shows that there are three kinds of term contributing to the time-dependent molecular dipole moment. According to the matrix elements involved they are denoted as bound-bound, bound-continuum, and continuum-continuum contributions. It should be noted that any one of the above contributions by itself is not an observable and

their relative strength (and with it our understanding of the mechanism of HHG) depends on the gauge chosen for the description of the problem (see Ref. [11] for a detailed discussion). Our specific choice of the length gauge in Eq. (6) is supposed to help in providing a simple physical picture of the molecular HHG.

The bound-bound terms describe the HHG due to transitions between the bound molecular states. Their overall population is limited by ionization. Under conditions of low ionization probability the strength of the bound-bound contribution is determined by the values of the transition dipole moments between the bound states. If the interaction with the field is described in the length gauge, the transition dipole moments between the ground and the first few excited states can be of the order of the molecular dimensions, i.e., much larger than the corresponding atomic ones. Thus, the importance of the bound-bound transitions for molecular HHG in this picture is much greater than in the atomic case. Indeed, in rare gas atoms they affect only the lower-energy part of the HHG spectra where the photon energy is smaller than the ionization energy, which means that the excitation energy of an atom is transferred to the emitted field. For alkali-metal atoms used in the experiment of Sheehy *et al.* [12] and possessing larger transition dipole moments the bound-bound contribution is much more significant. With molecules, one can get into the regime of high interaction energy (higher than the ionization energy). The bound-bound contribution to the molecular HHG can be viewed then as a transformation of the interaction energy into the energy of the emitted field.

The bound-continuum contribution is the dominant one for the high harmonics emitted by atoms. The well-known mechanism of atomic HHG due to Corkum and Kulander *et al.* [13,14] includes ionization, “free” motion of an electron in the electromagnetic field, and recombination. It is based on the existence of electronic trajectories that start after ionization not far from the nucleus with almost zero velocity and return to the vicinity of the nucleus to recombine. Such trajectories do not exist with circular polarization of the field, which leads to fast damping of the atomic HHG with increasing ellipticity (see, for example, Ref. [15]). The spatial periodicity of an electron trajectory is determined by the parameter $\alpha_0 = eE_0/m\omega^2$, where E_0 is the field strength and ω is the field frequency. This parameter represents the radius of the electron’s rotation at zero drift. If α_0 is much larger than the molecular size, the situation is similar to that in atoms and the bound-continuum contribution is expected to be small. For higher-frequency, lower-intensity fields, α_0 can become comparable to the radius of a small organic molecule, like benzene. In this case the notion of a “free” electron trajectory loses its relevance since for such fields the corresponding ponderomotive energy does not exceed the ionization energy of a molecule.

Finally, the transitions between the continuum states lying sufficiently high above the ionization threshold do not contribute to HHG, as has been shown by Ivanov and Rzażewski [16]. Within the dipole approximation, this can be under-

stood classically as a lack of harmonic emission by a “free” electron interacting with the electric component of the incident plane wave.

Substitution of the expansion (9) into the Schrödinger equation (6) provides coupled equations for the amplitudes $a_j(t)$ and $b(\vec{p}, t)$:

$$\begin{aligned} i\hbar\dot{a}_j(t) &= E_j a_j(t) - \sum_{j'=1}^{\infty} \langle \phi_j | e\vec{E}(t) \cdot \vec{r} | \phi_{j'} \rangle a_{j'}(t) \\ &\quad - \int_{-\infty}^{\infty} \frac{d^3 p}{(2\pi\hbar)^3} \langle \phi_j | e\vec{E}(t) \cdot \vec{r} | \varphi_{\vec{p}} \rangle b(\vec{p}, t), \quad (11) \\ i\hbar\dot{b}(\vec{p}, t) &= \frac{p^2}{2m} b(\vec{p}, t) - \int_{-\infty}^{\infty} \frac{d^3 p'}{(2\pi\hbar)^3} \\ &\quad \times \langle \varphi_{\vec{p}} | e\vec{E}(t) \cdot \vec{r} | \varphi_{\vec{p}'} \rangle b(\vec{p}', t) \\ &\quad - \sum_{j'=1}^{\infty} \langle \varphi_{\vec{p}} | e\vec{E}(t) \cdot \vec{r} | \phi_{j'} \rangle a_{j'}(t). \end{aligned}$$

The first of Eqs. (11) describes the transitions between the bound eigenstates of the molecular Hamiltonian [second term on the right-hand side (rhs)] and the ionization (the inhomogeneous third term on the rhs). The second equation provides the modification of the continuum eigenstates by the field (second term on the rhs). The inhomogeneity in the second equation is a source term describing the electrons appearing in the continuum.

Even under restrictions on the molecular symmetry and orientation, Eqs. (11) still depend on the energy level structure and the transition dipole moments of a specific system. Their exact solution can be obtained only numerically. In order to construct a general approximate theory of molecular HHG in the presence of N th-order DS catching the common features of the process, we resort to some severe approximations. In the next section we will calculate the bound-bound contribution in the high interaction energy limit generalizing the two-level theory of Ivanov and Corkum [17] to the case of N levels. The bound-continuum contribution will be estimated in the flat continuum approximation used in the atomic case by Lewenstein *et al.* [18].

III. A MODEL FOR THE BOUND-BOUND CONTRIBUTION

In order to estimate the bound-bound contribution to HHG one has to obtain the expressions for the bound state amplitudes. Consider the first of the equations (11). Suppose that the degree of ionization of the molecule due to its interaction with the time-dependent electric field is small and the term containing the amplitudes of the continuum states can be dropped in the zeroth-order approximation. Of the bound states, the most important for HHG are those that are coupled most efficiently [12]. In the case of a system possessing N th-order rotational symmetry such states form a complete basis for the representation of the rotation operator \hat{C}_N . For a single electron moving in a symmetric multicenter potential these are the first N molecular orbitals. For a real mol-

ecule, like benzene, these would be six multielectron states coupled by the single electron (e.g., π - π^*) transitions [20]. The equations for the amplitudes of N essential states are of the form

$$i\hbar\dot{a}_j(t) = E_j a_j(t) - \sum_{j'=0}^{N-1} \langle \phi_j | e \vec{E}(t) \cdot \vec{r} | \phi_{j'} \rangle a_{j'}(t),$$

$$j=0, \dots, N-1. \quad (12)$$

Suppose that the energy of interaction with the field is much larger than the energy differences between the molecular states. Within this approximation the details of the molecular energy level structure become unimportant and the N bound state energies can be assumed to be equal to the minus ionization energy of the system, $-I_p$. Under the above assumptions, the coupled equations governing the bound state populations are [compare to Eq. (12)]

$$i\hbar\dot{a}_j(t) = -I_p a_j(t) - \sum_{j'=0}^{N-1} \langle \phi_j | e \vec{E}(t) \cdot \vec{r} | \phi_{j'} \rangle a_{j'}(t).$$

$$(13)$$

Let us choose the electric field to be

$$\vec{E}(t) = E_0 [-\cos(\omega t), \sin(\omega t), 0]. \quad (14)$$

Then the interaction energy can be written in cylindrical coordinates as

$$e \vec{E}(t) \cdot \vec{r} = -\frac{1}{2} e E_0 \rho (e^{i\varphi} e^{i\omega t} + e^{-i\varphi} e^{-i\omega t}). \quad (15)$$

The molecular states ϕ_j can be chosen to be eigenstates of \hat{C}_N :

$$\hat{C}_N \phi_j = e^{-i2\pi j/N} \phi_j, \quad j=0, \dots, N-1. \quad (16)$$

In such a case, the dipole transitions are possible only between states with adjacent j 's:

$$\langle \phi_j | \rho e^{\pm i\varphi} | \phi_{j'} \rangle = d_{j,j'}^{\pm} \delta_{j, \text{mod}(j' \mp 1, N)}. \quad (17)$$

In the following we will assume that all the transition dipole moments are of the same magnitude

$$d_{j,j'}^{\pm} \approx \rho_0, \quad (18)$$

where ρ_0 is the molecular radius. The above assumption is valid when the overlap between the neighboring atomic orbitals is small. It allows us to obtain an exact solution for the system of equations (12) by a unitary transformation from the basis of eigenstates of rotation to the basis of localized states,

$$\psi_k = \frac{1}{\sqrt{N}} \sum_{j=0}^{N-1} e^{i2\pi jk/N} \phi_j, \quad k=0, \dots, N-1, \quad (19)$$

where the state ψ_k is localized around the nucleus found at the polar angle $2\pi k/N$. The coefficients of the localized states, \vec{c} , are related to those of the eigenstates of rotation, \vec{a} , by

$$c_k = \frac{1}{\sqrt{N}} \sum_{j=0}^{N-1} e^{i2\pi jk/N} a_j, \quad k=0, \dots, N-1, \quad (20)$$

$$a_j = \frac{1}{\sqrt{N}} \sum_{k=0}^{N-1} e^{-i2\pi jk/N} c_k, \quad j=0, \dots, N-1.$$

The transformation to the ψ_k basis diagonalizes the d^+ and d^- matrices simultaneously and leaves invariant the eigenenergy matrix due to the assumption of degeneracy of the N delocalized states. The decoupled equations for the amplitudes of the localized states c_k read

$$i\hbar\dot{c}_k(t) = -I_p c_k(t) - e E_0 \rho_0 \cos\left(\omega t + \frac{2\pi k}{N}\right) c_k(t),$$

$$k=0, \dots, N-1. \quad (21)$$

The general solution of equations (21) gives rise to N degenerate quasienergy states:

$$\Psi_{\alpha}(\vec{r}, t) = \sum_{k=0}^{N-1} c_{\alpha,k}(t) \psi_k(\vec{r}),$$

$$c_{\alpha,k}(t) = \frac{1}{\sqrt{N}} e^{iI_p t/\hbar} e^{i2\pi \alpha k/N} e^{i(e E_0 \rho_0/\hbar \omega) \sin(\omega t + 2\pi k/N)}, \quad (22)$$

where $\alpha=0, \dots, N-1$ is the Floquet state index.

The approximation obtained for the coefficients of the bound states is zeroth order in the energy splittings. If used in a direct calculation of the time-dependent dipole moment according to Eqs. (10) and (20), it would give zero result due to the assumed degeneracy. In order to overcome this difficulty, one can calculate the time derivative of the dipole moment using an expression that takes into account the energy level splittings [17]. The Fourier decompositions of the two quantities are related in a simple way:

$$\dot{\mu}_{\pm}(n\omega) = i n \omega \mu_{\pm}(n\omega). \quad (23)$$

The expression for the bound-bound part of $\dot{\mu}_{\pm}(t)$ via the amplitudes of the localized states $c_k(t)$ cannot be obtained directly from the Schrödinger equation (21), because the transformation to the localized state basis assumed degeneracy. Instead, one has to express the time derivative of the dipole moment via the coefficients of the delocalized states $a_j(t)$ and then use the transformation (20).

The components of the bound-bound part of the dipole moment can be represented via $a_j(t)$'s using the relations (17,18)

$$\mu_-^{b-b}(t) = e\rho_0 \sum_{j=0}^{N-1} a_{j+1}^*(t)a_j(t), \quad \mu_+^{b-b}(t) = [\mu_-^{b-b}(t)]^*. \quad (24)$$

The time derivative of the above expression can be expressed in terms of the coefficients of the delocalized states using the Schrödinger equation, which takes into account the exact eigenenergies of the delocalized states:

$$i\hbar \dot{a}_j(t) = E_j a_j(t) + \frac{eE_0\rho_0}{2} (e^{i\omega t} a_{j-1}(t) + e^{-i\omega t} a_{j+1}(t)). \quad (25)$$

The result reads (for brevity, here and throughout the rest of this section the superscript “*b-b*” will be omitted from the designation of the bound-bound part of the induced dipole moment)

$$\dot{\mu}_-(t) = i\dot{\mu}_0 \sum_{j=0}^{N-1} \frac{\omega_{j+1,j}}{\omega_{\text{int}}} a_{j+1}^*(t)a_j(t), \quad \dot{\mu}_+(t) = \dot{\mu}_-^*(t), \quad (26)$$

where $\dot{\mu}_0 = e\rho_0\omega_{\text{int}}$, $\omega_{\text{int}} = e\rho_0 E_0/\hbar$ is the frequency related to the interaction energy and $\omega_{j,j'} = (E_j - E_{j'})/\hbar$ are the Bohr frequencies of the system. Assuming Hückel energies

$$E_j = -2\beta \cos(2\pi j/N), \quad (27)$$

and using the transformation (20), one can express the time-dependent dipole moment derivative through the localized state coefficients:

$$\dot{\mu}_-(\vec{c}) = -2\dot{\mu}_0 \epsilon \sum_{k=0}^{N-1} e^{i(\pi/N)(2k+1)} \text{Im}(c_{k+1}^* c_k). \quad (28)$$

The magnitude of the first derivative of the dipole moment is related to two parameters, $\dot{\mu}_0$ and $\epsilon = \omega_0/\omega_{\text{int}}$, where $\omega_0 = 2\beta \sin(\pi/N)/\hbar$ is the frequency related to the level spacings. Since the level spacings were neglected in the zeroth order, ϵ is the natural perturbation strength parameter of the theory. Substituting the zeroth-order solution (22) into Eq. (28), one obtains the time dependence of $\dot{\mu}_-$:

$$\begin{aligned} \dot{\mu}_-(t) = & -\frac{2\dot{\mu}_0 \epsilon}{N} \sum_{k=0}^{N-1} e^{i(\pi/N)(2k+1)} \\ & \times \sin\left[\frac{2eE_0\rho_0}{\hbar\omega} \sin\left(\frac{\pi}{N}\right)\right] \\ & \times \cos\left(\omega t + \frac{\pi}{N}(2k+1)\right) - \frac{2\pi\alpha}{N}. \end{aligned} \quad (29)$$

The result (29), being proportional to the first power of ϵ , is the first-order approximation for the time-dependent dipole moment derivative. Its Fourier transform reads

$$\begin{aligned} \dot{\mu}_-(n\omega) = & 2\dot{\mu}_0 \epsilon (-1)^{n+l} \sin\left(\frac{2\pi\alpha}{N} + \frac{\pi n}{2}\right) \\ & \times J_n\left[2 \sin\left(\frac{\pi}{N}\right) \frac{eE_0\rho_0}{\hbar\omega}\right] \delta_{n,lN-1}. \end{aligned} \quad (30)$$

The spectrum of the dipole moment derivative component $\dot{\mu}_+(t) = \dot{\mu}_-^*(t)$ can be obtained using the relation

$$\dot{\mu}_+(n\omega) = \dot{\mu}_-^*(-n\omega). \quad (31)$$

By virtue of the property of Bessel functions, the HHG cut-off in the first-order approximation is

$$n_{\text{cutoff}}^{(1)} = \text{Int}\left\{\frac{eE_0 2 \sin(\pi/N)\rho_0}{\hbar\omega}\right\}, \quad (32)$$

where the expression $\text{Int}\{x\}$ means “integer of the form $lN \pm 1$ closest to x .” One can easily see that the length parameter $2 \sin(\pi/N)\rho_0$ appearing in Eq. (32) is the interatomic distance, in complete similarity to the result of Ref. [19] for HHG by a one-dimensional periodic structure perturbed by a linearly polarized field. Consequently, at first order the cutoff appears to be independent of the molecular size. However, this contradicts the simple physical intuition suggesting that at high enough field strength the bound-bound contribution to the HHG spectrum is a transformation of the interaction energy to that of the emitted harmonics. Indeed, the maximal variation of the interaction energy is related to the molecular radius ρ_0 and not to the interatomic distance [see Eq. (15)]. This contradiction makes it necessary to consider higher-order approximations for the molecular HHG spectrum. The standard way to achieve this goal is to obtain the further approximations for the time-dependent coefficients of the molecular bound states contributing to a given Floquet state, as mentioned in Ref. [17]. We, on the other hand, find it simpler to construct the higher-order approximations for the harmonic intensities in the following fashion. Consider the higher- (p th-) order derivatives of the time-dependent dipole moment $\mu_{\pm}^{(p)}(t)$, $p \geq 1$. Using the relation (24), they can be expressed via the time derivatives of the coefficients of the bound states:

$$\mu_{\pm}^{(p)}(t) = e\rho_0 \sum_{j=0}^{N-1} \sum_{q=0}^p C_q^p a_{j+1}^{(p-q)*} a_j^{(q)}, \quad \mu_+^{(p)}(t) = \mu_-^{(p)*}(t), \quad (33)$$

where C_q^p are the binomial coefficients. The derivatives $a_j^{(q)}$ can be expressed via the coefficients a_j themselves using the Schrödinger equation (25) which includes the energy spacings between the bound states. The amplitudes of these states are related in a known way to those of the localized states $c_k(t)$, [see Eq. (20)]. Substitution of the zeroth-order localized states coefficients into the exact expressions for the higher-order derivatives of the dipole moment allows one to take into account to a greater extent the neglected energy splittings of the bound states. The Fourier components of the higher-order derivatives are related to those of the dipole moment itself in a simple way:

$$\mu_{\pm}^{(p)}(n\omega) = (in\omega)^p \mu_{\pm}(n\omega). \quad (34)$$

The outlined procedure for the calculation of the higher-order approximations to the Fourier series of the bound-bound contribution to the dipole moment is analogous to the procedure already used by us for the calculation of the first-order approximation. Let us present here the results of the second- and third-order approximations. The second derivative expressed through the bound state coefficients takes on the following appearance:

$$\begin{aligned} \ddot{\mu}_{-}(\vec{a}) = & -\ddot{\mu}_0 \left[\sum_{j=0}^{N-1} \left(\frac{\omega_{j+1,j}}{\omega_{\text{int}}} \right)^2 a_{j+1}^*(t) a_j(t) \right. \\ & + \frac{\omega_{j+1,j}}{2\omega_{\text{int}}} \{ e^{-i\omega t} [|a_j|^2 - |a_{j+1}|^2] \\ & \left. + e^{i\omega t} (a_{j+2}^* a_j - a_{j-1} a_j^*) \} \right], \quad (35) \\ \ddot{\mu}_{+}(\vec{a}) = & \ddot{\mu}_{-}^*(\vec{a}), \end{aligned}$$

where $\ddot{\mu}_0 = e\rho_0\omega_{\text{int}}^2$. Upon transformation to the localized basis, $\ddot{\mu}_{\pm}(\vec{c})$ read

$$\begin{aligned} \ddot{\mu}_{-}(\vec{c}) = & -\ddot{\mu}_0 \sum_{q=-2,q \neq 0}^2 \sum_{k=0}^{N-1} \epsilon^{|q|} \ddot{\mu}_{-,q,k} c_k^* c_{k+q}, \\ \ddot{\mu}_{+}(\vec{c}) = & \ddot{\mu}_{-}^*(\vec{c}), \quad (36) \end{aligned}$$

where the coefficients $\ddot{\mu}_{-,q,k}$ are given by

$$\begin{aligned} \ddot{\mu}_{-, \pm 1, k} = & e^{-i\omega t} \sin\left(\frac{\pi}{N}\right) - \frac{i}{2} e^{i\omega t} e^{i4\pi k/N} (e^{\mp i\pi/N} - e^{\mp i3\pi/N}), \\ \ddot{\mu}_{-, \pm 2, k} = & -e^{i2\pi(k \pm 1)/N}. \quad (37) \end{aligned}$$

The Fourier decomposition of the second derivative of the dipole moment component is of the form

$$\begin{aligned} \ddot{\mu}_{-}(t) = & -\ddot{\mu}_0 \sum_{l=-\infty}^{\infty} \left(\epsilon^2 J_{lN-1} \left[2 \sin\left(\frac{2\pi}{N}\right) \frac{\omega_{\text{int}}}{\omega} \right] A_l \right. \\ & + \epsilon \left\{ J_{lN} \left[2 \sin\left(\frac{\pi}{N}\right) \frac{\omega_{\text{int}}}{\omega} \right] B_l \right. \\ & \left. \left. + J_{lN-2} \left[2 \sin\left(\frac{\pi}{N}\right) \frac{\omega_{\text{int}}}{\omega} \right] C_l \right\} \right) e^{i(lN-1)\omega t}, \quad (38) \end{aligned}$$

where the coefficients A_l, B_l , and C_l are given in Appendix A. The second derivatives of the dipole moment components contain contributions up to the second order in ϵ . The cutoff of the second order is located at

$$n_{\text{cutoff}}^{(2)} = \frac{eE_0 2 \sin(2\pi/N) \rho_0}{\hbar \omega}, \quad N \neq 4. \quad (39)$$

In the case of a three-center system ($N=3$), the second-order cutoff coincides with the first-order one, which suggests that the HHG of the system is described well already by the first-order approximation. In the case of $N=4$ the contribution of the second order in ϵ vanishes for all the quasienergy states $\alpha=0, \dots, N-1$ [see Eq. (A1)]. However, the cancellation of the second-order contribution for the four-level system is a property of Hückel energies (27) leading in this case to equal level spacings. In the general case of a four-level system possessing two degenerate levels ($\omega_{2,1}=0$) and unequal Bohr frequencies ($\omega_{0,1} \neq \omega_{3,2}$), the second-order cutoff is still given by Eq. (39) with $N=4$.

The expression for the third-order derivative of the dipole moment via the delocalized state coefficients \vec{a} is given in Appendix B. It contains contributions up to the third order in ϵ . The expressions for the higher derivatives as functions of the bound state amplitudes [e.g., Eqs. (35), (B1)] become progressively more cumbersome. Their use for the computation of the HHG spectra is not preferable over the numerical solution of the Schrödinger equation (25). However, they can be used for the prediction of the correct cutoff frequency. To this end, let us exploit the following line of reasoning. The p th-order derivatives of the dipole moment $\mu_{\pm}^{(p)}$ are quadratic forms in the bound state amplitudes a_j . After transformation to the localized basis they become quadratic forms in the localized state amplitudes c_k ,

$$\mu_{\pm}^{(p)} = \mu_0^{(p)} \sum_{k=0}^{N-1} \sum_{q=-p, q \neq 0}^p \epsilon^{|q|} \mu_{\pm, q, k}^{(p)} c_k^* c_{k+q}, \quad (40)$$

where $\mu_0^{(p)} = e\rho_0\omega_{\text{int}}^p$. According to the zeroth-order solution (22), the products of the localized state coefficients are of the general form

$$c_k^* c_{k+q} \propto \exp\left(i \frac{2 \sin \theta_q e E_0 \rho_0}{\hbar \omega} \cos(\omega t + \phi_0)\right), \quad (41)$$

where $\theta_q = q\pi/N$. The Fourier transform of such a product at the frequency $n\omega$ is proportional to Bessel function $J_n(eE_0\rho_0 \sin \theta_q / \hbar \omega)$, leading to a cutoff at $n_{\text{cutoff}} = eE_0\rho_0 \sin \theta_q / \hbar \omega$. For example, in the case of the first derivative only the adjacent localized states were coupled in the corresponding expression. This led to the cutoff of Eq. (32). The highest-order term present in the expressions for p th-order derivatives is

$$\sum_{j=0}^{N-1} \left(\frac{\omega_{j+1,j}}{\omega_{\text{int}}} \right)^p a_{j+1}^* a_j \quad (42)$$

[see Eqs. (26), (35), (B1)], which upon transformation to the localized basis couples c_k and $c_{k'}$ such that $k-k' = -p, \dots, p$. This means that by calculating the high enough dipole moment derivative one couples all the localized state amplitudes, unless the highest-order term vanishes (as in the case of $N=4$ for the Hückel model). Moreover, in order to achieve the coupling of all the N amplitudes, one has to go to the derivative of order $p=N/2$ or $p=(N+1)/2$ for even or odd symmetry orders, respectively. This fact has two important implications. First

of all, the ultimate cutoff position corresponds to $\max\{\sin[(k-k')\pi/N]\}$, where $k, k'=0, \dots, N-1$ [see Eq. (41)]. This gives

$$n_{\text{cutoff}}^{\text{even}} = \text{Int} \left\{ 2 \frac{eE_0\rho_0}{\hbar\omega} \right\} \quad (43)$$

for even symmetry orders and

$$n_{\text{cutoff}}^{\text{odd}} = \text{Int} \left\{ 2 \sin \left(\frac{(N-1)\pi}{2N} \right) \frac{eE_0\rho_0}{\hbar\omega} \right\} \quad (44)$$

for odd symmetry orders. Thus, the ultimate cutoff position for even N 's is exactly at the maximal variation of the interaction energy, while even for moderate odd N 's the difference between the corresponding cutoff position (44) and the interaction energy variation is quite small. If the first symmetry-allowed harmonic happens to be of order higher than n_{cutoff} of Eq. (43) or Eq. (44), the HHG spectrum consists of fundamental frequency only.

The second important conclusion is that in order to reproduce the HHG spectrum and in particular the cutoff position in a satisfactory way, one has to compute the time derivative of the dipole moment of order equal to half the symmetry order of the problem. For example, computing the third time derivative would be sufficient for the HHG spectrum of benzene ($N=6$) but not for species of higher-order symmetry. Going beyond the minimal order of perturbation theory needed for the correct prediction of the cutoff can change the calculated intensities of the emitted harmonics, but not the predicted cutoff position itself.

Analysis of expressions of the type (26), (35) and (B1) yields the structure of the HHG spectrum of our model in the plateau region. The higher plateau harmonics originating from terms of the type (42) are higher order in the small parameter of the theory, ϵ . This implies that the harmonic strengths in the plateau decrease with increasing order and at large enough values of the interaction energy the spectrum breaks into several plateaus each corresponding to a different order of the small parameter.

There are two kinds of exception from the general conclusions presented above. The first kind is related to the specific choice of energies, such as the absence of the second-order contribution for the Hückel four-level system. It has a clear physical significance, showing the effect of the energy structure of the unperturbed system on HHG. The second kind of deviation has to do with the extra symmetries appearing for specific quasienergy states (specific α 's) and leading to disappearance of series of harmonics from the HHG spectra or to cancellations of the contributions of specific orders. These effects are artifacts of the theory, which is based on the zeroth-order approximation to the localized state amplitudes.

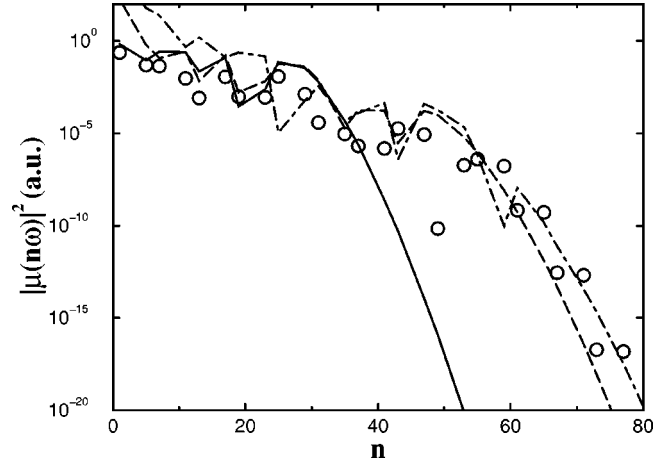


FIG. 1. HHG spectra of benzene model at superstrong field, $E_0=0.4$ a.u., for $\alpha=4$ quasienergy state. Solid line, first-order approximation; dashed line, second-order approximation; dash-dotted line, third-order approximation; circles, numerical results. The approximate analytical results obey the exact selection rule, but are designated by the lines for clarity. No scaling factors are introduced.

Let us now compare the analytical theory of the bound-bound contribution to the HHG spectra of N -center systems described above to numerical calculations based on the Schrödinger equation (25). Consider the six-level model of the benzene molecule ($N=6$), possessing a radius equal to the interatomic distance: $\rho_0=d_{C-C}=2.673$ a.u. The value of Hückel β [see Eq. (27)] for benzene according to the work of Pariser [21] is equal to 2.371 eV $\approx 8.717 \times 10^{-2}$ a.u. The field frequency chosen in our calculations is $\omega=0.037$ a.u. (≈ 1 eV). For the most detailed comparison of the analytical theory to the numerical calculations we would like to consider first a superintense field $E_0=0.4$ a.u. (corresponding to the intensity $I \approx 5.6 \times 10^{15}$ W/cm²). At such a field intensity the value of ϵ is about 0.085 and all the features of the HHG spectrum discussed above should be clearly manifested. The HHG spectra originating from the first-, second-, and third-order approximations are shown in Fig. 1 along with the numerical results. One can see that the first-order plateau appears in the exact spectrum at $n=eE_0d_{C-C}/\hbar\omega \approx 29$ as a step. The second plateau appearing due to the contributions of higher orders in ϵ is about three orders of magnitude lower. The ultimate cutoff is reproduced almost exactly by the third-order approximation at $n=61$ ($n_{\text{cutoff}}^{\text{even}}=2eE_0\rho_0/\hbar\omega \approx 58$). The deviations of the second- and especially the third-order approximations for the low-order harmonics from the numerical results are quite significant. This is related to the fact that the low-frequency Fourier components of the higher derivatives of the dipole moment are small. In order to reproduce the low-frequency part of the spectrum of the dipole itself, we divide them by the appropriate power of the field frequency according to Eq. (34). In the example considered, the frequency of the electric field is also small, $\omega < \omega_0$, which leads to the observed loss of precision.

In order to define the range of intensities feasible for the benzene HHG experiment we would like to refer to the re-

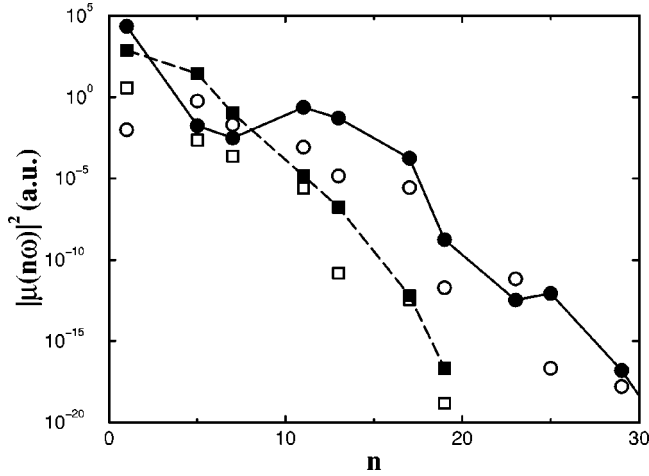


FIG. 2. HHG spectra of benzene model at moderate fields: full circles, $E_0=0.1$ a.u. (third-order approximation); empty circles, $E_0=0.1$ a.u. (numerical results); full squares, $E_0=0.05$ a.u. (third-order approximation); empty squares, $E_0=0.05$ a.u. (numerical results). The approximate harmonic intensities are joined by solid ($E_0=0.1$ a.u.) or dashed ($E_0=0.05$ a.u.) lines for better distinction between them and the corresponding numerical results.

cent work of Hankin *et al.* [22]. In this paper measurements of the saturation intensities of a series of organic molecules were reported. It has been found that the saturation intensity of benzene is just below 10^{14} W/cm². Although in the HHG experiment of Hay *et al.* benzene was exposed to intensities up to 5×10^{15} W/cm², the authors were not sure that the measured harmonic signal came from the molecules that experienced the peak intensity [23,24]. The bound-bound contributions to the HHG spectrum of benzene at the field strengths of 0.05 a.u. and 0.1 a.u. (corresponding to intensities of about 8.8×10^{13} W/cm² and 3.5×10^{14} W/cm², respectively) are shown in Fig. 2. At the lower intensity the cutoff appears at $n=7$, in agreement with the prediction (43). Accordingly, only one pair of harmonics ($n=5,7$) appears in the plateau region. At the higher intensity, two pairs of plateau harmonics ($n=5,7,11,13$) are followed by the cutoff at $n_{\text{cutoff}}^{\text{even}}=14$. It should be pointed out that the absolute values of the Fourier components of the bound-bound part of the dipole moment are much higher than those usually predicted for the bound-continuum transitions in rare gas atoms [25].

IV. A MODEL FOR THE BOUND-CONTINUUM CONTRIBUTION

The estimation of the bound-continuum contribution to the time-dependent dipole moment is based on the approximate solution of the Schrödinger equation for the continuum state amplitudes. We would like to rewrite the Schrödinger equation for the coefficients of the continuum states [the second of Eqs. (11)] using the approximation of N degenerate bound states. As in the previous section, this approximation allows us to use the localized state basis $\{\psi_k\}$:

$$i\hbar \dot{b}(\vec{p}, t) = \frac{p^2}{2m} b(\vec{p}, t) - \int_{-\infty}^{\infty} \frac{d^3 p'}{(2\pi\hbar)^3} \langle \varphi_{\vec{p}} | e^{\vec{E}(t) \cdot \vec{r}} | \varphi_{\vec{p}'} \rangle b(\vec{p}', t) - \sum_{k=0}^{N-1} \langle \varphi_{\vec{p}} | e^{\vec{E}(t) \cdot \vec{r}} | \psi_k \rangle c_k(t), \quad (45)$$

where the electric field $\vec{E}(t)$ is given by Eq. (14).

In order to solve Eqs. (45) coupling different continuum states let us employ the flat continuum approximation. Within this approximation the field-free continuum eigenfunctions corresponding to the energies $p^2/2m$ are represented by plane waves:

$$\varphi_{\vec{p}} = e^{i\vec{p} \cdot \vec{r} / \hbar}. \quad (46)$$

The approximation (46) has been applied to the calculation of atomic HHG by Lewenstein and co-workers [18]. It is expected to work well when the Coulomb interaction of the ionized electron with the core is much weaker than its interaction with the electric field over the larger part of the electron trajectory. The flat continuum approximation allows one to decouple Eqs. (45) (see Ref. [18]):

$$i\hbar \dot{b}(\vec{p}, t) = \frac{p^2}{2m} b(\vec{p}, t) - e^{\vec{E}(t) \cdot \vec{r}} i\hbar \vec{\nabla}_{\vec{p}} b(\vec{p}, t) - \sum_{k=0}^{N-1} e^{\vec{E}(t) \cdot \vec{r}} \vec{d}_k(\vec{p}) c_k(t), \quad (47)$$

where $\vec{d}_k(\vec{p}) = \langle \varphi_{\vec{p}} | \vec{r} | \psi_k \rangle$ is the bound-continuum transition dipole moment. The Schrödinger equation (47) can be solved exactly by means of the substitution

$$b(\vec{p}, t) = e^{e\vec{A}(t) \cdot \vec{\nabla}_{\vec{p}}} \tilde{b}(\vec{p}, t), \quad (48)$$

where $\vec{A}(t) = -\int^t \vec{E}(t') dt'$ is the vector potential. The resulting solution reads

$$b(\vec{p}, t) = \frac{i}{\hbar} \sum_{k=0}^{N-1} \int_0^t e^{\vec{E}(t') \cdot \vec{r}} \vec{d}_k[\vec{p} + e\vec{A}(t) - e\vec{A}(t')] c_k(t') \times \exp\left(-\frac{i}{\hbar} \int_{t'}^t \frac{[\vec{p} + e\vec{A}(t) - e\vec{A}(t'')]^2}{2m} dt''\right) dt'. \quad (49)$$

The integration constant in the solution (49) is chosen in such a way that the continuum state amplitudes are zero at the time $t=0$. Using the flat continuum approximation for the amplitudes $b(\vec{p}, t)$, we obtain the following expression for the bound-continuum part of the induced dipole moment [compare to the second term on the rhs of Eq. (10)]:

$$\begin{aligned} \vec{\mu}^{b-c} = & 2e \operatorname{Re} \left\{ \frac{i}{\hbar} \sum_{j=0}^{N-1} \sum_{k=0}^{N-1} \int_0^t dt' \int_{-\infty}^{\infty} \frac{d^3 P}{(2\pi\hbar)^3} c_j^*(t) \right. \\ & \times \vec{d}_j^*[\vec{P} - e\vec{A}(t)] \exp \left(-\frac{i}{\hbar} \int_{t'}^t \frac{[\vec{P} - e\vec{A}(t'')]^2}{2m} dt'' \right) \\ & \left. \times e\vec{E}(t') \cdot \vec{d}_k[\vec{P} - e\vec{A}(t')] c_k(t') \right\}, \end{aligned} \quad (50)$$

where $\vec{P} = \vec{p} + e\vec{A}(t)$ is the canonical momentum. The above expression can be viewed as a generalization of the formula derived by Lewenstein and co-workers for the bound-continuum part of the induced dipole moment [18] to the case of N bound states. The interpretation of Eq. (50) is analogous to that of the corresponding single bound state (atomic) expression. At the time t' the electron makes a transition from the localized state ψ_k to the continuum state characterized by the kinematic momentum $\vec{p} = \vec{P} - e\vec{A}(t')$. The term $c_k(t') e\vec{E}(t') \cdot \vec{d}_k[\vec{P} - e\vec{A}(t')]$ is associated with the probability amplitude of this transition. The electron propagates under the influence of the electric field only from the time t' to the time t . The time-dependent part of the corresponding classical action, $-\int_{t'}^t [\vec{P} - e\vec{A}(t'')]^2/2m dt''$, enters the exponential term. The analogous term in the single bound state expression of Lewenstein and co-workers contains the energy of the initial state, $-I_p$, as well. In Eq. (50), on the other hand, it is contained in the bound state amplitudes. The recombination of electrons into the localized state ψ_j takes place at the time t . The related probability amplitude is associated with $\vec{d}_j^*[\vec{P} - e\vec{A}(t)] c_j^*(t)$. In this section we will estimate the bound-continuum part of the time-dependent dipole moment using approximate transition dipole moments and localized state coefficients.

In order to introduce a specific function for the transition dipole moments $\vec{d}_j(\vec{p})$, we would like to employ the Gaussian model, namely, to approximate the localized wave functions ψ_j by Gaussians:

$$\begin{aligned} \psi_j = & \left(\frac{1}{\sqrt{\pi} r_0} \right)^{3/2} e^{-|\vec{r} - \vec{r}_j|^2/2r_0^2}, \\ \vec{r}_j = & \rho_0 \left[\cos\left(\frac{2\pi j}{N}\right), \sin\left(\frac{2\pi j}{N}\right), 0 \right]. \end{aligned} \quad (51)$$

The parameter r_0 defines the width of the localized wave function. It should not exceed $|\vec{r}_j - \vec{r}_{j'}|/\sqrt{2}$ for our approximation for the bound-bound transitions dipole moments to hold [see Eq. (18)]. Too small values of r_0 , on the other hand, would indicate the lack of chemical bonding. Within the Gaussian model (51), the bound-continuum transition dipole moments are:

$$\vec{d}_j(\vec{p}) = \frac{\hbar}{i} (2\sqrt{\pi} r_0)^{3/2} e^{-r_0^2 |\vec{p}|^2/2\hbar^2} e^{-(i/\hbar) \vec{p} \cdot \vec{r}_j} \left(\frac{r_0^2}{\hbar^2} \vec{p} + \frac{i}{\hbar} \vec{r}_j \right). \quad (52)$$

For the evaluation of the integral over canonical momenta in Eq. (50) it is convenient to divide the $\vec{d}_j(\vec{p})$ functions into the fast oscillating and slowly changing factors:

$$\vec{d}_j(\vec{p}) = e^{-(i/\hbar) \vec{p} \cdot \vec{r}_j} \vec{d}_j^t(\vec{p}). \quad (53)$$

Using the above notation, the expression for the bound-continuum part of the dipole moment can be rewritten as

$$\begin{aligned} \vec{\mu}^{b-c} = & 2e \operatorname{Re} \left\{ \frac{i}{\hbar} \sum_{j=0}^{N-1} \sum_{k=0}^{N-1} \int_0^t dt' \int_{-\infty}^{\infty} \frac{d^3 P}{(2\pi\hbar)^3} \right. \\ & \times c_j^*(t) \vec{d}_j^*[\vec{P} - e\vec{A}(t)] \exp \left[\frac{i}{\hbar} \left([\vec{P} - e\vec{A}(t)] \cdot \vec{r}_j \right. \right. \\ & \left. \left. - [\vec{P} - e\vec{A}(t')] \cdot \vec{r}_k - \int_{t'}^t \frac{[\vec{P} - e\vec{A}(t'')]^2}{2m} dt'' \right) \right] \\ & \left. \times e\vec{E}(t') \cdot \vec{d}_k[\vec{P} - e\vec{A}(t')] c_k(t') \right\}. \end{aligned} \quad (54)$$

Note that the oscillating exponential term in Eq. (54) is of the form $\exp[iS_{\text{cl}}(\vec{P}, t, t')/\hbar]$, where $S_{\text{cl}}(\vec{P}, t, t')$ is the classical action change along the trajectory starting at the point \vec{r}_k at time t' and ending at the point \vec{r}_j at time t . This “free” electron trajectory is characterized by a constant value of the canonical momentum \vec{P} (corresponding to the drift motion of the electron).

The integration over \vec{P} in the expression for the bound-continuum part of the dipole moment can be performed by the stationary phase method [18]. The corresponding stationary phase condition is

$$\vec{\nabla}_{\vec{P}} S_{\text{cl}}(\vec{P}, t, t') \Big|_{\vec{P} = \vec{p}_{\text{st}}} = \vec{r}_j - \vec{r}_k - \frac{1}{m} \int_{t'}^t [\vec{P}_{\text{st}} - e\vec{A}(t'')] dt'' = 0. \quad (55)$$

The physical meaning of Eq. (55) is that the electron removed by the field from the k th site should return to the j th site in order to recombine. Consequently, only the returning trajectories give rise to HHG. Noting that for the harmonic fields [as in Eq. (14)] $\int^t \vec{A}(t') dt' = \vec{E}(t)/\omega^2$, we find the stationary momentum to be equal to

$$\vec{P}_{\text{st}}(t, t') = \frac{m(\vec{r}_j - \vec{r}_k) + (e/\omega^2)[\vec{E}(t) - \vec{E}(t')]}{t - t'}. \quad (56)$$

After stationary phase integration over \vec{P} , the expression (54) takes on the following appearance:

$$\begin{aligned}
\vec{\mu}^{b-c} = & 2e \operatorname{Re} \left\{ \frac{i}{\hbar} \sum_{j=0}^{N-1} \sum_{k=0}^{N-1} \int_0^t dt' c_j^*(t) \vec{d}'_j^* [\vec{P}_{\text{st}} - e\vec{A}(t)] \right. \\
& \times \left(\frac{-im}{2\pi\hbar(t-t')} \right)^{3/2} \exp \left[\frac{i}{\hbar} \left([\vec{P}_{\text{st}} - e\vec{A}(t)] \cdot \vec{r}_j \right. \right. \\
& \left. \left. - [\vec{P}_{\text{st}} - e\vec{A}(t')] \cdot \vec{r}_k - \int_{t'}^t \frac{[\vec{P}_{\text{st}} - e\vec{A}(t'')]^2}{2m} dt'' \right) \right] \\
& \left. \times e\vec{E}(t') \cdot \vec{d}'_k [\vec{P}_{\text{st}} - e\vec{A}(t')] c_k(t') \right\}. \quad (57)
\end{aligned}$$

The bound state amplitudes involved in the above expression can be rewritten in terms of the vector potential [compare to Eq. (22)]:

$$c_j(t) = \frac{1}{\sqrt{N}} e^{iI_p t/\hbar} e^{i2\pi\alpha k/N} e^{-(i/\hbar)e\vec{A}(t) \cdot \vec{r}_j}. \quad (58)$$

Substitution of the coefficients c_j into Eq. (57) leads to the following result:

$$\begin{aligned}
\vec{\mu}^{b-c} = & 2e \operatorname{Re} \left\{ \frac{i}{\hbar} \frac{1}{N} \sum_{j=0}^{N-1} \sum_{k=0}^{N-1} e^{i2\pi\alpha(k-j)/N} \int_0^t d\tau \right. \\
& \times \vec{d}'_j^* [\vec{P}_{\text{st}} - e\vec{A}(t)] \left(\frac{-im}{2\pi\hbar\tau} \right)^{3/2} \exp \left\{ \frac{i}{\hbar} \left[\vec{P}_{\text{st}} \cdot (\vec{r}_j - \vec{r}_k) \right. \right. \\
& \left. \left. - \int_{t-\tau}^t \left(\frac{[\vec{P}_{\text{st}} - e\vec{A}(t'')]^2}{2m} + I_p \right) dt'' \right] \right\} \\
& \left. \times e\vec{E}(t-\tau) \cdot \vec{d}'_k [\vec{P}_{\text{st}} - e\vec{A}(t-\tau)] \right\}, \quad (59)
\end{aligned}$$

where the change of variables $\tau = t - t'$ has been made. The oscillating exponential term of the integrand of Eq. (59) comprises the so-called quasiclassical action $S_{\text{qcl}} = S_{\text{cl}} - I_p \tau$ appearing in Landau-Dykhne type expressions for adiabatic transition probabilities [18,26].

The integration over τ in Eq. (59) can be performed either by the saddle point method or numerically. In any case, it is worthwhile to discuss the corresponding stationary phase condition:

$$\begin{aligned}
\frac{dS_{\text{qcl}}}{d\tau} = & \left(\frac{\partial S_{\text{qcl}}}{\partial \tau} \right)_{\vec{P}_{\text{st}}} + \vec{\nabla}_{\vec{P}_{\text{st}}} S_{\text{qcl}} \cdot \frac{\partial \vec{P}_{\text{st}}}{\partial \tau} = \left(\frac{\partial S_{\text{qcl}}}{\partial \tau} \right)_{\vec{P}_{\text{st}}} \\
= & - \left(\frac{[\vec{P}_{\text{st}} - e\vec{A}(t-\tau)]^2}{2m} + I_p \right) = 0. \quad (60)
\end{aligned}$$

As one can see, the condition (60) is identical to the one arising in the atomic case [18,27]. For characteristic field

parameters, like those considered in Sec. III, the kinetic energy of electron rotational motion [ponderomotive energy, $U_p = e^2 E_0^2 / (2m\omega^2)$] is substantially larger than the typical molecular ionization potential. In such a case the ionization energy in Eq. (60) can be neglected. Then, the physical meaning of the stationary phase condition is that the electron possesses zero velocity at the moment of ionization, $\vec{v}(t-\tau) = [\vec{P}_{\text{st}} - e\vec{A}(t-\tau)]/m = 0$. Thus, the classical trajectories important for the bound-continuum contribution are those starting at the k th atom with zero velocity and arriving at the j th atom after time $\tau = \tau_{\text{st}}$. Classical trajectories of electrons in a circularly polarized field are characterized by the radius of rotational motion $\alpha_0 = eE_0 / (m\omega^2)$ and the drift velocity $\vec{v}_d = \vec{P}/m$. For small polyatomic molecules interacting with intense light, the former parameter is typically much larger than the molecular dimensions, $\alpha_0 \gg \rho_0$. Simple kinematic considerations lead to the conclusion that under such a constraint the kinetic energy at the moment of recombination is just a small fraction of the ponderomotive energy (see Appendix C). Consequently, the bound-continuum contribution to the generation of high harmonics is expected to be small.

Let us note in passing that an interesting classical trajectory of another kind arising in the context of the molecular interaction with circularly polarized radiation is the “resonant” trajectory with zero drift and $\alpha_0 = \rho_0$. For small molecules the corresponding ponderomotive energy would be insufficient for such a trajectory to be thought of as “free,” $U_p = eE_0\rho_0/2 < I_p$. However, it might have relevance for larger structures, like nanotubes [6]. Quantum mechanically speaking, the resonant trajectory is associated with continuum-continuum transitions, not leading perhaps to efficient HHG. It can be of importance for multiphoton ionization processes if the lifetime of the corresponding resonance state is sufficiently long.

In the present work we employ numerical integration over τ in order to calculate the bound-continuum contribution to the time-dependent dipole moment (59). The relations (14) and (55) are used in order to express the quasiclassical action S_{qcl} as a function of time:

$$\begin{aligned}
S_{\text{qcl}}(t, \tau) = & \frac{m\rho_0^2}{\tau} \sin^2 \left(\frac{\pi}{N}(j-k) \right) - (U_p + I_p)\tau \\
& + \frac{4eE_0\rho_0}{\omega^2\tau} \sin \left(\frac{\omega\tau}{2} \right) \sin \left(\frac{\pi}{N}(j-k) \right) \\
& \times \cos \left(\omega t - \frac{\omega\tau}{2} + \frac{\pi}{N}(j+k) \right). \quad (61)
\end{aligned}$$

The integrand of Eq. (59) possesses an essential singularity at $\tau=0$ for $j \neq k$ due to the term $\exp(-iS_{\text{qcl}}/\hbar)$. From the physical point of view, this singular point corresponds to recombination at the j th site zero time after the ionization from the k th site. Within the nonrelativistic theory presented here, approaching the singularity would require either superhigh electric fields or superhigh initial velocities of the ionized electron. Consequently, the $\tau=0$ point can be excluded from the integration range and the integral over τ in the

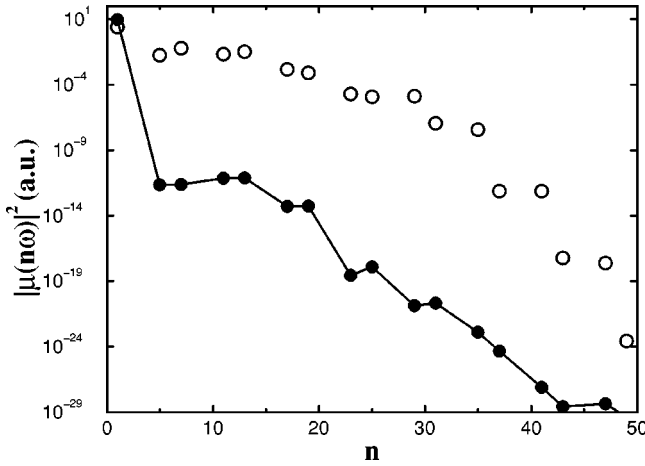


FIG. 3. Bound-bound (empty circles) and bound-continuum (full circles and continuous line) contributions to the HHG spectrum of the $N=6$ system at $E_0=0.2$ a.u.

formula for the bound-continuum part of the dipole moment should be understood as $\int_{\eta}^t d\tau \dots$, where $\eta \rightarrow +0$. In practice, the lower integration limit should be much smaller than the time it takes an electron to recombine, $\eta \ll 2\sqrt{\rho_0/\alpha_0}/\omega$ (see Appendix C).

The bound-bound and bound-continuum contributions to HHG by the six bound levels, flat continuum system ($I_p = 0.340$ a.u., $r_0 = 1.3$ a.u.) are compared in Fig. 3. The numerical results were found to be stable to changes in τ below $\tau = 10^{-3}T$, $T = 2\pi/\omega$. One can see that the bound-continuum contribution is by several orders of magnitude weaker than the bound-bound one. This could be explained already by the assumption of low continuum state population lying at the basis of our theory. Our numerical results show that the cutoff of the bound-continuum part of $\mu_{\pm}(n\omega)$ is identical to that of the bound-bound part [i.e., it is given by Eqs. (43), (44)]. The bound-continuum cutoff position can be explained by noting that the corresponding contribution to the dipole moment comes from small τ 's: $\tau \leq 2\sqrt{\rho_0/\alpha_0}/\omega \ll 2\pi/\omega$ (see Appendix C). For such small time differences between the ionization and the recombination, the time dependence of the quasiclassical action is

$$S_{\text{qcl}}(t) \sim \frac{2eE_0\rho_0}{\omega} \sin\left(\frac{\pi}{N}(j-k)\right) \cos\left(\omega t + \frac{\pi}{N}(j+k)\right). \quad (62)$$

The cutoff of the Fourier transform of $\exp[iS_{\text{qcl}}(t)/\hbar]$ is indeed identical to the cutoff of the bound-bound contribution (43), (44). Moreover, it does not depend linearly on the ponderomotive energy, but rather scales as the interaction energy. Thus, the bound-continuum contribution to molecular HHG in circular polarization cannot be viewed as a transformation of the kinetic energy of the ionized electron to the energy of the emitted photon.

V. CONCLUSIONS

We have presented a general theory of HHG by a symmetric N -center system lying in the polarization plane of a

circularly polarized field. We have found that in the length gauge the bound-bound contribution to the time-dependent dipole moment is much bigger than the bound-continuum one, which is natural in the considered regime of low continuum population. Moreover, the cutoffs of both contributions were found to coincide. Thus, the whole HHG spectrum of the class of systems considered is dominated by the harmonics emitted due to transitions between the bound states. The HHG cutoff is shown to be at the maximal variation of the interaction energy (43) and (44). The cutoff position leads to the interpretation of the HHG process as the transformation of the interaction energy into the energy of the emitted harmonics. This mechanism is qualitatively different from the rescattering process responsible for HHG in the atomic case [13,14]. The key parameters defining the cutoff energy are the electric field strength and the molecular radius. The former parameter cannot be increased indefinitely due to the onset of strong ionization beyond the saturation intensity. The latter parameter, however, can serve as an efficient lever to control the HHG spectrum. The molecular size dependence of the ionization probability should be taken into account in this respect [28,29]. In the frequency region of 1 eV and below, the multielectron effects can play the dominant role in multiphoton ionization of large molecules. Their saturation intensities can be sufficiently higher than the single-active-electron predictions [30].

At present, the results of the present work cannot be compared directly to the experimental ones because there is no evidence for a very efficient molecular alignment in the current strong field experiments with symmetric molecules. It is very interesting, however, to confront our theory with the experiment by Hay *et al.* [23,24]. The high efficiency (comparable to that of Xe) of benzene HHG in the plateau region found by the authors may stem from the efficient population of the excited bound states, similarly to the situation in gaseous alkali metals [12]. The reported nonuniform behavior of the harmonic signals as functions of intensity [23] in the longer pulse experiment does not persist at the shorter pulse length [24] and thus is attributed by the authors to fragmentation of the molecules. The ellipticity dependences of the 7th and 11th harmonics generated in benzene (both harmonics are symmetry allowed for molecules oriented in the polarization plane of the field) show at least an order of magnitude decrease of the harmonic intensities at increasing ellipticity. However, these measurements were performed using the longer pulses of peak intensity of 3×10^{15} W/cm², i.e., under conditions of efficient fragmentation. The authors report no results of ellipticity dependence measurements with shorter pulses [24].

Trying to look at the recent experimental results from the point of view of the developed theory, one notices two important directions of further theoretical research. First, the theoretical framework suggested in this paper is by no means limited to the circular polarization case. Its generalization to an arbitrary field and an arbitrary molecular orientation is straightforward and should be able to explain the relative intensity of HHG by benzene, cyclohexane, and Xe found by Hay *et al.* and to verify the extent of the applicability of the rescattering model to molecular HHG. Second, the macroscopic response of a molecular gas should be investigated,

first with the assumption of a perfect molecular alignment with the field polarization plane and then in the general case.

Finally, we would like to point out that the significance of our theoretical results is not limited to gas phase molecular HHG. Due to the lack of importance of bound-continuum transitions in the case considered, the theory could be relevant for solid state targets as well. For example, in Ref. [6] we considered HHG by arrays of parallel single-walled carbon nanotubes interacting with a circularly polarized beam that propagates along the nanotube axes. The time-dependent tight-binding model solved by us numerically for the calculation of nanotube HHG predicts cutoff positions close to the maximal variation of the interaction energy. However, the absolute intensities of the high harmonics vary appreciably with the nanotube structure, e.g., they are different for “zig-zag” and “armchair” nanotubes of similar diameters. Analysis of the nanotube HHG along the lines of Sec. III would lead to a better understanding of the dependence of the HHG spectra on the unperturbed energy level structures of various types of nanotube.

ACKNOWLEDGMENTS

This work was supported in part by the Israel-U.S. BSF, by the Basic Research Foundation administered by the Israeli Academy of Sciences and Humanities, and by the Fund for the Promotion of Research at Technion. The authors would like to thank Professor L. S. Cederbaum, Dr. M. Yu. Ivanov, Professor E. E. Nikitin, and Professor U. Peskin for fruitful discussions.

APPENDIX A: A , B , AND C COEFFICIENTS IN THE FOURIER DECOMPOSITION OF $\ddot{\mu}_-$

The coefficients entering the expression (38) for the Fourier decomposition of the second derivative of the dipole moment component $\ddot{\mu}_-$ are

$$A_l = 2 i^{lN-1} \begin{cases} \cos\left(\frac{2\pi}{N}(2\alpha + lN)\right), & lN \text{ is even} \\ -i \sin\left(\frac{2\pi}{N}(2\alpha + lN)\right), & lN \text{ is odd,} \end{cases}$$

$$B_l = 2 i^{lN} \sin\left(\frac{\pi}{N}\right) \begin{cases} \cos\left(\frac{2\pi\alpha}{N}\right), & lN \text{ is even} \\ -i \sin\left(\frac{2\pi\alpha}{N}\right), & lN \text{ is odd,} \end{cases} \quad (\text{A1})$$

$$C_l = 2 i^{lN-1} \sin\left(\frac{\pi}{N}\right) \begin{cases} \sin\left(\frac{2\pi}{N}(\alpha - 1)\right), & lN \text{ is even} \\ i \cos\left(\frac{2\pi}{N}(\alpha - 1)\right), & lN \text{ is odd.} \end{cases}$$

APPENDIX B: THE THIRD TIME DERIVATIVE OF THE DIPOLE MOMENT AS A FUNCTION OF THE BOUND STATE AMPLITUDES

The third time derivative of the induced dipole moment of an N -center system can be expressed through the bound state amplitudes a_j in the same way as is done for the first [Eq. (26)] and second [Eq. (35)] derivatives. The resulting expression reads

$$\begin{aligned} \mu_-^{(3)} = & -i\mu_0^{(3)} \sum_{j=0}^{N-1} \left\{ \left(\frac{\omega_{j+1,j}}{\omega_{\text{int}}} \right)^3 a_{j+1}^* a_j \right. \\ & + \frac{1}{2} \left(\frac{\omega_{j+1,j}}{\omega_{\text{int}}} \right)^2 \left[e^{-i\omega t} (a_{j+2}^* a_j - a_{j+1}^* a_{j-1}) \right. \\ & + e^{i\omega t} \left(|a_j|^2 - |a_{j+1}|^2 + \frac{\omega_{j+2,j}}{\omega_{j+1,j}} a_{j+2}^* a_j - a_{j+1}^* a_{j-1} \right) \left. \right] \\ & + \frac{1}{4} \frac{\omega_{j+1,j}}{\omega_{\text{int}}} \left[2i e^{-i\omega t} \text{Im}(e^{-i\omega t} a_{j-1}^* a_j \right. \\ & - e^{i\omega t} a_{j+2}^* a_{j+1}) + 2a_{j+1}^* a_j - a_{j+2}^* a_{j+1} - a_j^* a_{j-1} \\ & + 4i e^{i\omega t} \text{Im}(e^{i\omega t} a_{j+1}^* a_j) + e^{2i\omega t} (a_{j+3}^* a_j - a_{j+2}^* a_{j-1} \\ & \left. \left. - a_{j+1}^* a_{j-1} + a_{j+1}^* a_{j-2}) \right] \right\}, \quad (\text{B1}) \end{aligned}$$

where $\mu_0^{(3)} = e\rho_0\omega_{\text{int}}^3$.

APPENDIX C: KINEMATICS OF THE STATIONARY PHASE TRAJECTORIES AT LARGE α_0

The “free” electron trajectories starting with zero velocity at the k th atom at time t' are given by

$$\begin{aligned} x(t) = & \alpha_0 [\cos(\omega t) - \cos(\omega t')] + v_0 \sin(\omega t')(t - t') \\ & + \rho_0 \cos\left(\frac{2\pi k}{N}\right), \\ y(t) = & -\alpha_0 [\sin(\omega t) - \sin(\omega t')] + v_0 \cos(\omega t')(t - t') \\ & + \rho_0 \sin\left(\frac{2\pi k}{N}\right), \quad (\text{C1}) \\ v_x(t) = & v_0 [\sin(\omega t') - \sin(\omega t)], \\ v_y(t) = & v_0 [\cos(\omega t') - \cos(\omega t)], \end{aligned}$$

where $\alpha_0 = eE_0/(m\omega^2)$ and $v_0 = eE_0/(m\omega)$. At the time t the trajectory should arrive at the j th atom:

$$x(t) = \rho_0 \cos\left(\frac{2\pi j}{N}\right), \quad y(t) = \rho_0 \sin\left(\frac{2\pi j}{N}\right). \quad (\text{C2})$$

Substituting Eqs. (C2) into Eqs. (C1) and eliminating the drift terms proportional to $t - t' = \tau$, one obtains

$$\cos(\omega\tau) = \frac{\rho_0}{\alpha_0} \left[\cos\left(\frac{2\pi j}{N} + \omega t'\right) - \cos\left(\frac{2\pi k}{N} + \omega t'\right) \right] + 1, \quad (\text{C3})$$

where $\rho_0/\alpha_0 \ll 1$. Consequently, the time difference between the ionization and recombination, τ , is also small. Expansion of $\cos(\omega\tau)$ in a Taylor series leads to

$$\tau \leq \frac{2}{\omega} \sqrt{\frac{\rho_0}{\alpha_0}}. \quad (\text{C4})$$

The electron kinetic energy at the moment of recombination is

$$\begin{aligned} E_{\text{kin}} &= \frac{mv_x^2(t)}{2} + \frac{mv_y^2(t)}{2} = mv_0^2 [1 - \cos(\omega\tau)] \leq 2mv_0^2 \frac{\rho_0}{\alpha_0} \\ &= 4 \frac{\rho_0}{\alpha_0} U_p \ll U_p. \end{aligned} \quad (\text{C5})$$

Thus, the recombination does not lead to the generation of high-order harmonics.

-
- [1] P. Salières, A. L'Huillier, P. Antoine, and M. Lewenstein, *Adv. At., Mol., Opt. Phys.* **4**, 83 (1999); T. Brabec and F. Krausz, *Rev. Mod. Phys.* **72**, 745 (2000).
- [2] Z. Chang, A. Rundquist, H. Wang, M.M. Murnane, and H.C. Kapteyn, *Phys. Rev. Lett.* **79**, 2967 (1997); M. Schnürer, Ch. Spielmann, P. Wobrauschek, C. Strelt, N.H. Burnett, C. Kan, K. Ferencz, R. Koppitsch, Z. Cheng, T. Brabec, and F. Krausz, *ibid.* **80**, 3236 (1998).
- [3] A. Rundquist, C.G. Durfee III, Z. Chang, C. Herne, S. Backus, M.M. Murnane, and H.C. Kapteyn, *Science* **280**, 1412 (1998); Y. Tamaki, J. Itatani, Y. Nagata, M. Obara, and K. Midorikawa, *Phys. Rev. Lett.* **82**, 1422 (1999); E. Constant, D. Garzella, P. Breger, E. Mével, Ch. Dorrer, C. Le Blanc, F. Salin, and P. Agostini, *ibid.* **82**, 1668 (1999).
- [4] M. Gisselbrecht, D. Descamps, C. Lyngå, A. L'Huillier, C.-G. Wahlström, and M. Meyer, *Phys. Rev. Lett.* **82**, 4607 (1999).
- [5] O.E. Alon, V. Averbukh, and N. Moiseyev, *Phys. Rev. Lett.* **80**, 3743 (1998).
- [6] O.E. Alon, V. Averbukh, and N. Moiseyev, *Phys. Rev. Lett.* **85**, 5218 (2000).
- [7] F.H.M. Faisal, *Theory of Multiphoton Processes* (Plenum, New York, 1986).
- [8] R. Bavli and H. Metiu, *Phys. Rev. A* **47**, 3299 (1993).
- [9] J.J. Larsen, I. Wendt-Larsen, and H. Stapelfeldt, *Phys. Rev. Lett.* **83**, 1123 (1999); J.J. Larsen, H. Sakai, C.P. Safvan, I. Wendt-Larsen, and H. Stapelfeldt, *J. Chem. Phys.* **111**, 7774 (1999); J.J. Larsen, K. Hald, N. Bjerre, and H. Stapelfeldt, *Phys. Rev. Lett.* **85**, 2470 (2000).
- [10] S.-I. Chu and X.-M. Tong, *Phys. Rev. A* **58**, R2656 (1998); V. Averbukh, O.E. Alon, and N. Moiseyev, *ibid.* **60**, 2585 (1999).
- [11] C. Figueira de Morisson Faria, M. Dörr, and W. Sandner, *Phys. Rev. A* **58**, 2990 (1998).
- [12] B. Sheehy, J.D.D. Martin, L.F. DiMauro, P. Agostini, K.J. Schafer, M.B. Gaarde, and K.C. Kulander, *Phys. Rev. Lett.* **83**, 5270 (1999).
- [13] P.B. Corkum, *Phys. Rev. Lett.* **71**, 1994 (1993).
- [14] K. Kulander, K. Schafer, and J. Krause, in *Super-Intense Laser-Atom Physics*, Vol. 316 of *NATO Advanced Study Institutes, Series B: Physics*, edited by B. Piraux, A. L'Huillier, and K. Rzażewski (Plenum, New York, 1993), p. 316.
- [15] N.H. Burnett, C. Kan, and P.B. Corkum, *Phys. Rev. A* **51**, R3418 (1995).
- [16] M.Yu. Ivanov and K. Rzażewski, *J. Mod. Opt.* **39**, 2377 (1992).
- [17] M.Yu. Ivanov and P.B. Corkum, *Phys. Rev. A* **48**, 580 (1993).
- [18] M. Lewenstein, Ph. Balcoup, M.Yu. Ivanov, A. L'Huillier, and P.B. Corkum, *Phys. Rev. A* **49**, 2117 (1994); P. Antoine, A. L'Huillier, M. Lewenstein, P. Salières, and B. Carré, *ibid.* **53**, 1725 (1996).
- [19] A.D. Bandrauk and A.A. Ovchinnikov, *Phys. Rev. B* **50**, 3473 (1994).
- [20] B.O. Roos, K. Anderson, and M.P. Fülischer, *Chem. Phys. Lett.* **192**, 5 (1992); J.E. Del Bene, J.D. Watts, and R.J. Bartlett, *J. Chem. Phys.* **106**, 6051 (1997).
- [21] R. Pariser, *J. Chem. Phys.* **24**, 250 (1956).
- [22] S.M. Hankin, D.M. Villeneuve, P.B. Corkum, and D.M. Rayner, *Phys. Rev. Lett.* **84**, 5082 (2000).
- [23] N. Hay, R. de Nalda, E. Springate, K.J. Mendham, and J.P. Marangos, *Phys. Rev. A* **61**, 053810 (2000).
- [24] N. Hay, R. de Nalda, T. Halfmann, K.J. Mendham, M.B. Mason, M. Castillejo, and J.P. Marangos, *Phys. Rev. A* **62**, 041803 (2000).
- [25] J.L. Krause, K.J. Schafer, and K.C. Kulander, *Phys. Rev. A* **45**, 4998 (1992).
- [26] N.B. Delone and V.P. Krainov, *Multiphoton Processes in Atoms*, 2nd ed., Vol. 13 of *Springer Series on Atoms and Plasmas* (Springer, Berlin, 2000).
- [27] D.B. Milošević, *J. Phys. B* **33**, 2479 (2000).
- [28] A. Talebpoor, S. Laroche, and S.L. Chin, *J. Phys. B* **31**, 2769 (1998).
- [29] M.J. DeWitt, and R.J. Levis, *Phys. Rev. Lett.* **81**, 5101 (1998).
- [30] M. Lezius, V. Blanchet, D.M. Rayner, D.M. Villeneuve, A. Stolow, and M.Yu. Ivanov, *Phys. Rev. Lett.* **86**, 51 (2001).